ELSEVIER

PII: S0032-3861(98)00153-0

Polymer Vol. 39 No. 25, pp. 6261–6268, 1998
© 1998 Elsevier Science Ltd
Printed in Great Britain. All rights reserved
0032-3861/98/$ - see front matter

Composition effects in polyetherurethane-based solid polymer electrolytes

Simon T. C. Ng[a], Maria Forsyth[a,*], Douglas R. MacFarlane[b], Maria Garcia[c], Mark E. Smith[c] and John H. Strange[c]

[a]*Department of Materials Engineering, Monash University, Clayton, Victoria 3168, Australia*

[b]*Department of Chemistry, Monash University, Clayton, Victoria 3168, Australia*

[c]*Department of Physics, University of Kent, Canterbury, Kent, CT2 7NR, UK*

(Revised 16 February 1998)

Nuclear magnetic resonance spectroscopy (n.m.r.), dynamic mechanical thermal analysis (d.m.t.a.) and AC impedance techniques have been used in combination to probe the effect of electrolyte composition in an archetypal solid polymer electrolyte (SPE). A series of solid polymer electrolytes (SPEs) based on a urethane-crosslinked trifunctional poly(ethylene glycol) polymer host containing dissolved ionic species ($LiClO_4$ and $LiCF_3SO_3$) have been studied. D.m.t.a. has established that increasing $LiClO_4$ concentration causes a decrease in the polymer segmental mobility, owing to the formation of transient crosslinks via cation–polymer interaction. Investigation of the distribution of mechanical/structural relaxation times for the $LiClO_4$/polymer complex with d.m.t.a. reveals that increasing $LiClO_4$ concentration causes a slight broadening of the distribution, indicating a more heterogeneous environment. Results of n.m.r. ^{7}Li T_1 and T_2 relaxation experiments support the idea that higher salt concentrations encourage ionic aggregation. This is of critical importance in determining the conductivity of the material since it affects the number of charge carriers available. Introduction of the plasticiser tetraglyme into the $LiClO_4$-based SPEs suppresses the glass transition temperature of the SPE, and causes a significant broadening of the relaxation time distribution (as measured by d.m.t.a.). © 1998 Elsevier Science Ltd. All rights reserved.

(Keywords: solid polymer electrolyte; ionic conductivity; polyether network)

INTRODUCTION

The concept of a solid polymer electrolyte (SPE) was first proposed by Wright *et al.*[1] and developed more fully by Armand *et al.*[2]. The study of SPEs has been continuing for some 15 to 20 years, during which time understanding of these materials has improved considerably. A number of comprehensive reviews have been published on the subject[3–6]. In SPEs ionic conduction takes place via the motion of dissolved ionic species through a solid polymeric medium[4]. Typical materials used include poly(ethylene oxide) (PEO), a semicrystalline polymer, and inorganic alkali metal salts. Other materials have come to the fore in recent years because of an improved understanding of the conduction mechanism[4–6].

SPEs are being developed for a variety of uses, including solid-state batteries[4] and electrochromic displays[7]. The current room-temperature conductivity achievable with these materials is of the order of 10^{-4} S cm^{-1}. This is at the lower end of the acceptable conductivity range for SPEs to find use in ambient-temperature electrochemical devices, but it is quite suitable for electrochromic applications[7].

Much work has been done to understand how the motion of ions occurs through the polymer host, and how the nature of the components of an SPE affects the motion and environment of the charge-carrying species. It is well established[8,9] that conduction occurs primarily in the amorphous component of the polymer and, as a result, research is now focused on amorphous materials as polymer hosts. The fully amorphous network elastomer studied here is based on an ethylene oxide/propylene oxide copolymer (3PEG) in which the random occurrence of pendant methyl groups serves to disrupt the chain symmetry sufficiently to diminish the extent of crystallinity and to lower the melting point of any crystalline regions to around −35°C.

The motion of the charge-carrying species is dependent upon molecular relaxation of the polymer host[3–6], with significant conduction only occurring above the glass transition temperature, T_g. Transport properties of the polymer electrolytes, such as conductivity, have often been shown to follow a Vogel–Tammann–Fulcher (VTF) temperature dependence, highlighting the importance of the polymer mobility in determining conductivity[6]. According to this model, the temperature-dependent conductivity, $\sigma(T)$, is given by[10]

$$\sigma = A \exp\left[-B/(T - T_0)\right] \quad (1)$$

where T_0 is an 'ideal' glass transition temperature (often taken as $T_g - 50$ K), and A and B are constants. By improving polymer mobility through careful selection of the polymer host and introduction of low-molecular-weight diluents to reduce T_g, one is therefore able to improve conductivity while still retaining adequate elastomeric mechanical properties.

Also of key significance in determining the conductivity of an SPE is the concentration of charge-carrying species. As a result of the low dielectric constant of most polymer

* To whom correspondence should be addressed

hosts, SPEs are weak electrolytes[4–6,11]. The presence of ionic aggregates[4–6,11–13] (solvent-separated pairs, contact pairs and higher combinations) results in a reduction in the number of charge-carrying species to values well below the completely dissociated limit.

To improve conductivity, it is necessary to understand how changing the nature and components of the SPE affect the level of salt aggregation, the molecular mobility within the polymer/salt complex and the mechanisms of motion of the charge-carrying species. Previous work by this group has looked specifically at the role of plasticisers in SPEs[14–22] and has shown that the mechanisms by which plasticisers improve conductivity are quite distinct and depend on the specific chemical nature of the plasticiser.

Recent nuclear magnetic resonance (n.m.r.) results[23] have also suggested the presence of at least two lithium species in both unplasticised and tetraglyme-plasticised $LiClO_4$/3PEG systems. Although the results are not yet conclusive, it may be that the short T_2 species are aggregates, while the long T_2 species are 'free' cations. The relative intensities of the two species changed with temperature, salt concentration and tetraglyme content. Dynamic mechanical thermal analysis (d.m.t.a.) experiments on $LiCF_3SO_3$/3PEG systems plasticised with tetraglyme[24] and polycarbonate (PC)[25] support the notion that plasticisers change the environment of the cation by changing the morphological homogeneity of the system.

The combination of AC impedance, d.m.t.a. and n.m.r. techniques is used in this paper, with an emphasis on the complementary information that can be derived, for an archetypal amorphous polyether system. In particular, the effect of electrolyte composition is used to probe the environment and dynamics of the charge-carrying species.

EXPERIMENTAL METHOD

Materials

A trifunctional poly(ethylene-*co*-propylene) glycol (3PEG), molecular weight 5000 g mol^{-1}, was purchased from ICI and dried under vacuum at 40°C for 72 h to remove all residual moisture. Lithium perchlorate ($LiClO_4$) and lithium triflate ($LiCF_3SO_3$) salts from Aldrich were dried under vacuum at 120°C for 48 h prior to use to remove excess moisture. Tetraglyme, purchased from Aldrich, was vacuum distilled over sodium metal to remove impurities. All components were stored under a dry N_2 atmosphere at room temperature.

Sample preparation

Stock solutions of fixed $LiClO_4$ or $LiCF_3SO_3$ concentrations were made by dissolving the required quantities of the salt into both 3PEG and tetraglyme under hot (323 K) stirring conditions in a dry N_2 atmosphere. Concentrations are expressed as moles of salt per kg of solvent (m), where solvent mass is taken to include both the masses of the polymer and plasticiser if both are present. To ensure the complete absence of moisture, the stock solution of polymer was redried under vacuum at 50°C for a period of 24 h prior to use. 3PEG discolours when exposed to heat and light for prolonged periods, and therefore care was taken not to expose it to light during the heating stage. From the stock solutions a range of samples of varying composition were made. The stock solutions were carefully mixed to ensure homogeneity, and then the crosslinking agent, diisocyanatohexane, was added in stoichiometric amounts to these stock solutions. Thorcat catalyst was added after the crosslinking agent had been stirred thoroughly into the mixture. Before the crosslinking reaction had progressed to any significant degree, the solution was poured into a Teflon mould. For d.m.t.a., the samples were cast into the shape of discs 2 mm thick and 10 mm in diameter, while for n.m.r. measurements, the samples were cylindrical in shape with a diameter of 8 mm and a length of 15 mm. Conductivity samples were made by pouring the mixture directly into the conductivity cell. The samples were then left to cure for 12 h at 310 K. A post-cure period of 2 days was allowed to ensure that the samples had reached equilibrium. Following this, all samples were visually inspected for bubbles and other defects that would have affected the measurements.

Nuclear magnetic resonance

^{7}Li relaxation times were measured at 29.876 MHz with a modified Bruker CXP spectrometer equipped with a superconducting magnet operating at approximately 1.79 T. A specially constructed probe with an 8 mm solenoidal coil capable of attaining temperatures in the range 77–1250 K was used. During experimentation, however, a temperature of 363 K was not exceeded in order to prevent plasticiser volatilisation or sample decomposition. T_1 relaxation times were determined by using an inversion-recovery pulse sequence and T_2 by the Hahn spin-echo pulse sequence. Single exponentials fit the magnetization decays for the T_1 experiments, suggesting a single T_1 in all cases. However, at lower temperatures, bi-exponential expressions were better able to fit the T_2 data, therefore suggesting the presence of two T_2 components. The $\pi/2$ pulse lengths for these experiments were of the order of 7 μs.

Dynamic mechanical thermal analysis

Measurements of the complex modulus of the samples as a function of temperature over the range $T_g - 40$ K to $T_g + 40$ K were made by using a Perkin–Elmer DMA7 dynamic mechanical thermal analyser. Samples were removed from the dry N_2 atmosphere and placed immediately into the d.m.t.a. apparatus. They were then cooled under a dry helium atmosphere at a rate of 20°C min^{-1} to the starting temperature, and held there for 5 min to allow thermal equilibration. Upon attaining thermal equilibrium, two parallel plates were used to apply a combined static (1000 mN) and sinusoidal ($\pm$ 900 mN) load to the samples, and the sample was heated at 2°C min^{-1} to the upper temperature limit. The strain response to the applied load was measured and recorded during this heating period. Data were analysed fully with the Perkin–Elmer DMA7 software. Glass transition temperatures and glass transition widths (full-widths at half-maximum) were determined.

Conductivity

Conductivity was measured over the temperature range 247 K to 353 K. Duplicate samples were cast to establish the reproducibility of the results. Conductivity measurements were made with a Hewlett–Packard Impedance Meter over a frequency range of 20 Hz to 1 MHz. Cole–Cole impedance plots were used to determine the 'touchdown' point, and thus the SPE resistance. The cell constant was determined by calibration with a 0.01 m KCl solution at 25°C both before and after the experiment to establish reproducibility.

RESULTS AND DISCUSSION

Dynamic mechanical thermal analysis

Figure 1 is a typical d.m.t.a. trace showing the storage

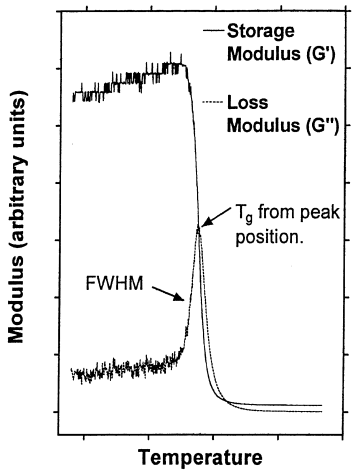

Figure 1 D.m.t.a. trace of storage modulus (G') and loss modulus (G''). T_g values are measured from the temperature position of the G'' peak maximum, with the width of the relaxation taken as the full-width at half-maximum of the G'' peak

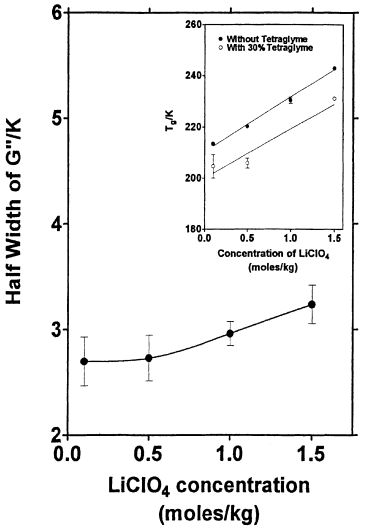

Figure 2 The G'' width (half-width at full-maximum) plotted as a function of $LiClO_4$ concentration in unplasticised 3PEG, showing a marginal increase in the distribution of polymer relaxation times as the salt concentration is increased. The inset is a plot of T_g as a function of $LiClO_4$ concentration in 3PEG and 3PEG/30 wt% tetraglyme samples. Error bars shown are the standard deviations determined from multiple experiments

(G') and loss modulus (G'') behaviour as a function of temperature. The ratio of G'' to G' is related to a value tan δ, where δ is the phase difference between the applied stress and the responding strain. This phase difference changes as the material undergoes the transition from a glassy to a rubbery state (the mechanical effect of T_g)[26]. T_g is determined from the maximum in the loss modulus (G'') peak, as marked in *Figure 1*. T_g values were measured for a range of samples with varying concentrations of $LiClO_4$ at zero and 30 wt% tetraglyme, and varying tetraglyme contents at 1.5 m salt content. The inset of *Figure 2* shows T_g as a function of salt concentration for unplasticised samples and those containing 30 wt% tetraglyme. In both cases T_g increases linearly with increasing salt concentration, this general trend being consistent with the formation of inter- and intramolecular transient crosslinks[27]. The T_g behaviour upon addition of 30 wt% tetraglyme shows a similar dependence on the salt concentration, but

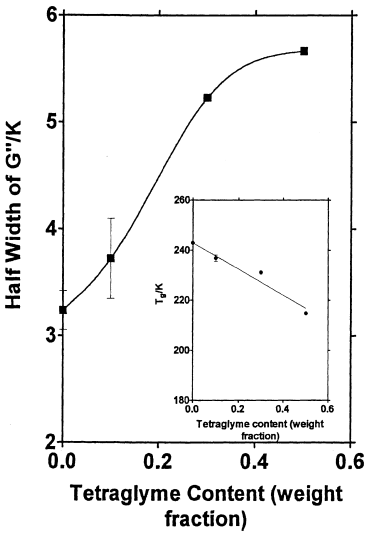

Figure 3 G'' width (full-width at half-maximum) plotted as a function of tetraglyme content in a 1.5 M $LiClO_4$/3PEG complex, with an increase in the level of plasticiser producing a marked broadening of the relaxation time distribution. The inset shows T_g as a function of tetraglyme content in a sample of fixed (1.5 m) $LiClO_4$ concentration. Error bars shown are the standard deviations determined from multiple experiments

with a uniform decrease in T_g due to the effect of tetraglyme as a plasticiser. *Figure 3* inset further demonstrates the plasticising effect of adding tetraglyme in varying quantities to a sample with constant salt concentration.

All of the samples examined by d.m.t.a. displayed a single T_g suggesting that, on the length scale probed by d.m.t.a. (100 Å), all samples consisted of a single phase[28]. The width of the glass transition is related to the distribution of relaxation times, and hence to the degree of homogeneity in the sample[26]. This behaviour is not inconsistent with the presence of a stretched exponential relaxation mechanism (as modelled by the Kolrausch–Williams–Watts (KWW) equation, for example) in which the stretching phenomenon may be explained by a distribution of relaxation times. Measurements of transition width were made by observing changes in the full-width at half-maximum (FWHM) of the loss modulus peak. *Figures 2* and *3* plot loss modulus peak FWHM against (1) salt concentration in unplasticised samples and (2) tetraglyme content in 1.5 m $LiClO_4$ samples. A small increase in width was observed as salt concentration rose from 0.1 m to 1.5 m, suggesting that increasing salt concentration only marginally influences the distribution of relaxation times in the polymer. In contrast, a significant increase in width is seen as the tetraglyme content is increased. Sukeshini *et al.*[29] have observed similar trends in a poly(vinyl chloride) (PVC)/plasticiser/Li bis(trifluoromethanesulfonyl)imide solid electrolyte (the plasticiser being either dibutyl phthalate or dioctyl adipate), where the loss modulus peak broadened with increasing levels of plasticiser, and eventually split into two peaks associated with a plasticiser-rich phase and a PVC-rich phase. Observations consistent with the formation of salt-rich phases as salt concentration is increased have also been made in poly(propylene oxide) (PPO)/$LiClO_4$ and amorphous PEO-1000/$LiClO_4$ complexes[30,31]. In contrast, the unplasticised samples of this work demonstrated only a small increase in width of the loss modulus peak with increasing salt concentration, suggesting that the distribution of motional correlation times remains constant despite the changing salt concentration. Therefore, the broadening

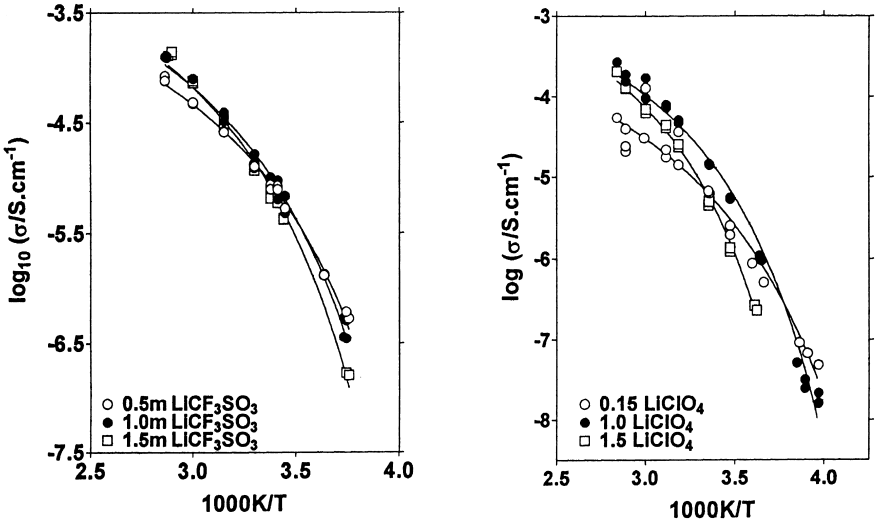

Figure 4 Conductivity temperature dependence as a function of (a) $LiClO_4$ concentration (0.15 m, 1.0 m and 1.5 m) and (b) $LiCF_3SO_3$ concentration (0.5 m, 1.0 m and 1.5 m) in 3PEG. Both curves exhibit temperature dependence typical of Vogel–Tammann–Fulcher behaviour, linking the mechanism of conductivity to relaxation governed by free volume or configurational entropy. The reproducibility is indicated by the duplicate measurements as indicated

Table 1 Vogel–Tammann–Fulcher (VTF) parameters (A, B, T_0) and activation energies (E_a) determined from conductivity for $LiClO_4$ and $LiCF_3SO_3$ samples using the VTF-derived equation. All errors listed are standard deviations determined from a least-squares fit of the appropriate equations

Technique	Sample	VTF parameters			E_a (kJ mol^{-1}) from equation (2)
		A	B (K)	T_0 (K)	
Conductivity	0.15 m $LiClO_4$	0.029 ± 0.01	1117 ± 61	169	40.9 ± 2.2
	1.0 m $LiClO_4$	0.32 ± 0.07	1170 ± 23	183	51.8 ± 1.0
	1.5 m $LiClO_4$	0.35 ± 0.07	1194 ± 22	192	60.4 ± 1.2
	0.5 m $LiCF_3SO_3$	0.033 ± 0.01	1080 ± 19	167	38.5 ± 1.0
	1.0 m $LiCF_3SO_3$	0.108 ± 0.02	1150 ± 20	174	44.9 ± 1.9
	1.5 m $LiCF_3SO_3$	0.198 ± 0.03	1195 ± 18	180	51.1 ± 2.8

of the loss modulus peak observed upon addition of tetraglyme is probably due to its heterogeneous distribution throughout the polymer host, although the pockets of tetraglyme seem not to be large enough to cause the splitting of the peak as observed in the PVC systems mentioned above, and as observed in PC-plasticised $LiCF_3SO_3$ systems[25].

Conductivity

Figure 4a and *b* shows conductivity behaviour as a function of reciprocal temperature for three $LiClO_4$- and three $LiCF_3SO_3$-based samples. The conductivity data display a VTF temperature dependence, and were modelled adequately by equation (1) with a fixed value of T_0 (taken to be $T_g - 50$ K). Similar temperature behaviour has been reported elsewhere for both $LiClO_4$ and $LiCF_3SO_3$ salts in amorphous SPEs[30,32,33]. The parameters determined from fitting of equation (1) (A and B) are given in *Table 1*. The interpretation of these parameters is model-dependent. Nevertheless, A can be related to the number of charge carriers within the system, and B to an activation process and critical configurational entropy or to a critical free volume[11,34].

The suitability of the VTF equation in fitting the data of *Figure 4* suggests that the mechanism facilitating charge-carrier motion involves molecular relaxation governed by free volume or configurational entropy. While this is generally accepted, a number of anomalies need to be addressed. In many cases, when the VTF model is used to fit conductivity data that are clearly non-Arrhenius, the values of a floating T_0 parameter (not used in this case) are often close to, if not greater than, the material T_g. It is generally accepted that the mechanism of conductivity is not solely governed by relaxation of the polymer host. Arumagum *et al.*[35] and Ferry *et al.*[36] have both pointed out a possible contributing mechanism for conduction involving not only a percolation of the cation between adjacent oxygens, but also a hopping mechanism involving the 'free' cations moving between aggregates. Ferry *et al.*[36] claim that this mechanism occurs predominantly at higher salt concentration. An interesting factor that may contribute to the shape of conductivity–temperature plots is the proportional decrease in the number of charge carriers occurring at higher temperatures, resulting in a relatively smaller increase of σ with temperature. Such observations of a temperature-dependent 'free ion' concentration have been made in SPEs[12,13,20], as well as being predicted theoretically for low-molecular-weight solvent systems[37], and could at least partially explain the additional curvature observed in some cases.

The relationship between conductivity and salt concentration is a complex one. Higher salt concentrations improve conductivity by increasing charge-carrier concentration, but also cause an increase in sample T_g. Consequently, at lower temperatures those samples with a higher salt concentration can have lower conductivities (*Figure 4*). A further

complication is the possibility that increasing salt concentration promotes ionic aggregation, as evidenced from Fourier transform infra-red (*FT*i.r.) spectroscopy[20]. This has implications in determining the relative importance of the two factors contributing to conductivity in SPEs—charge-carrier mobility and charge-carrier concentration. The addition of tetraglyme to a 1.5 m $LiClO_4$/3PEG sample has been shown to both decrease the T_g of the SPE (increasing the mobility within the system) and also to improve its conductivity[22]. While tetraglyme, a low-molecular-weight polyether with a dielectric constant similar to 3PEG, was not expected to play a significant role in influencing the level of dissociation of $LiClO_4$, there is evidence[20] that it promotes ionic aggregation in $LiCF_3SO_3$/3PEG complexes.

Activation energies (E_a) were calculated at 323 K for each of the conductivity curves by using the following relationship (equation (2)) and values of B presented in *Table 1*

$$\frac{E_a}{R} = \frac{T^2 B}{(T - T_0)^2} \tag{2}$$

where equation (2) was derived by assuming $E_a = \mathrm{d}(\ln \sigma)/\mathrm{d}(1/T)$ and differentiating the VTF equation (equation (1)). Wetton[38] claims this is a meaningful E_a, but the values derived approach infinity as T approaches T_0; in reality, this has not been observed to occur, the conductivity behaviour becoming Arrhenius near and below T_g.

E_a rises with concentration for both salt systems, but is consistently smaller in the $LiCF_3SO_3$ samples. The rise with increasing salt concentration is not unexpected given that ionic mobility diminishes as T_g becomes larger. The higher values of E_a in the $LiClO_4$ samples may be a result of the higher values of T_0 for these systems, a possible indication that greater levels of crosslinking occur due to differences in the level of ionic aggregation, or it may indeed reflect the presence of a conducting species which is inherently less mobile. The parameter B has been related via the configurational entropy theory to an activated process[34]. B undergoes a small but probably negligible increase with salt concentration in both cases—an observation which is consistent with results published by Boden and co-workers[34]. B is also unaltered by a change in anionic species. This invariance regardless of anion or concentration indicates that the activated process governing conductivity is similar in both systems, and that changing the salt concentration merely produces a shift in the position of T_0.

The pre-exponential term is, however, not invariant as a function of salt concentration or salt type. For both salt species A rises dramatically as the concentration is increased, but seems to approach a plateau in the $LiClO_4$ system. A is a complex quantity comprised of contributions from charge-carrier concentration and temperature[11,34]. It would appear that charge-carrier concentration increases towards a maximum as salt concentration rises in the case of $LiClO_4$, while for $LiCF_3SO_3$ the rise appears to be steady for the concentration range studied. Furthermore, a comparison of the values of A for the two salt systems indicates that a greater number of charge carriers is present in the $LiClO_4$-based samples.

Nuclear magnetic resonance

Basic n.m.r. theory. Bloembergen, Purcell and Pound (BPP)[39] developed a simple model to describe the correlation time dependence of the n.m.r. spin–lattice relaxation rate, based on the assumption of a single correlation time (τ_C) describing the Brownian motion of a nucleus relative to its environment. The spin–lattice relaxation between like spins I is

$$\frac{1}{T_1} = \frac{C_1}{r^6}\left[J(\omega_L) + J(2\omega_L)\right] \tag{3}$$

where $J(\omega_L)$ and $J(2\omega_L)$ are spectral density functions representing the density of fluctuations in the magnetic field (either magnetic or electric) at the Larmor frequency (ω_L) and twice the Larmor frequency ($2\omega_L$). The constant C_1 depends upon the nature of the spin interaction responsible for relaxation. According to the BPP model, based on the assumption of a single exponential correlation time (τ_C), the spectral density function is related to τ_C by

$$J(\omega_L) = \frac{\tau_C}{1 + \omega_L^2 \tau_C^2} \tag{4}$$

Furthermore, if the relaxation is attributed to a homonuclear dipolar interaction mechanism, the following expression for the spin–lattice relaxation results

$$\frac{1}{T_1} = \frac{C_1}{r^6}\left[\frac{\tau_C}{1 + \omega_L^2 \tau_C^2} + \frac{4\tau_C}{1 + 4\omega_L^2 \tau_C^2}\right] \tag{5}$$

with r as the distance between the centres of interaction. Spin–spin relaxation can be modelled similarly

$$\frac{1}{T_2} = \frac{C_2}{r^6}\left[3\tau_C + \frac{5\tau_C}{1 + \omega_L^2 \tau_C^2} + \frac{2\tau_C}{1 + 4\omega_L^2 \tau_C^2}\right] \tag{6}$$

In this case, there is a frequency-independent term, $3\tau_C$, which will dominate relaxation at low temperature for $\omega_L \tau_C \gg 1$. Consequently, T_2 is influenced by frequency-independent interactions.

Equations (5) and (6) can be expressed in temperature-dependent form by assuming a thermally activated process. An Arrhenius temperature dependence model for τ_C is often assumed, although in polymers there may be an argument for a VTF dependence[6], the choice to a large extent related to the nucleus being probed and its relationship with the host within which it resides. Chung *et al.*[40] found that ^{7}Li T_1 relaxation behaviour in poly(propylene glycol) was inadequately modelled when using a VTF-based τ_C temperature dependence—a reflection of the fact that τ_C is not obviously determined by free-volume- or configurational-entropy-related motions in their system.

A minimum occurs at $\omega_L \tau_C = 0.6158$; thus for a fixed ω_L, one can compare the relative mobilities of the nuclei in samples of differing composition by comparing the temperature positions of the minima. Minima occurring at higher temperatures indicate less mobile nuclei. Furthermore, the value of T_1 at the minimum is then only dependent upon the strength of the interaction (described by the prefactor in equation (3)), with variations in T_1 a result of changes in the interaction distance (r) or in the nature of the interaction itself (heteronuclear or quadrupolar, for example).

^{7}Li T_1 relaxation time experiments. ^{7}Li T_1 relaxation temperature-dependent measurements were made at 29.876 MHz for three $LiClO_4$ samples and three $LiCF_3SO_3$ samples. Results are shown in *Figure 5a* and *Figure 5b*, respectively.

Table 2 lists E_a as determined from *Figure 5* for $LiClO_4$ and $LiCF_3SO_3$, the values having been calculated from the limiting high- and low-temperature slopes of the relaxation

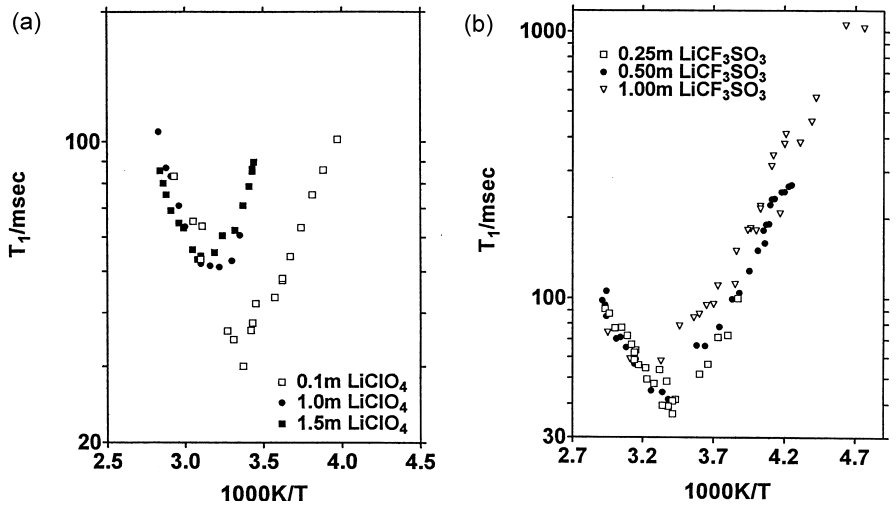

Figure 5 ^{7}Li T_1 relaxation behaviour for (a) 0.1 m, 1.0 m and 1.5 m $LiClO_4$/3PEG complexes and (b) 0.25 m, 0.5 m and 1.0 m $LiCF_3SO_3$/3PEG complexes as a function of inverse temperature. The value of T_1 at the minimum increases with salt concentration; an indicator of ionic aggregation. Error in the points is ± 5%

Table 2 Activation energies (E_a) determined from fitting an Arrhenius equation to the ^{7}Li T_1 n.m.r. relaxation measurements. All errors listed are standard deviations determined from least-squares fits of the appropriate equations

Technique	Sample	E_a (kJ mol^{-1})
N.m.r.	0.1 m LiClO4 (low temp.)	18.8 ± 1.5
	0.1 m $LiClO_4$ (high temp.)	20.2 ± 1.7
	1.0 m $LiClO_4$ (high temp.)	25.3 ± 1.5
	1.5 m $LiClO_4$ (low temp.)	25.7 ± 1.0
	1.5 m $LiClO_4$ (high temp.)	26.7 ± 1.2
	0.25 m $LiCF_3SO_3$ (low temp.)	15.8 ± 1.0
	0.25 m $LiCF_3SO_3$ (high temp.)	19.0 ± 4.0
	0.5 m $LiCF_3SO_3$ (low temp.)	19.7 ± 2.0 and 7.7 ± 2.0
	0.5 m $LiCF_3SO_3$ (high temp.)	19.1 ± 0.6
	1.0 m $LiCF_3SO_3$ (low temp.)	19.0 ± 2.0

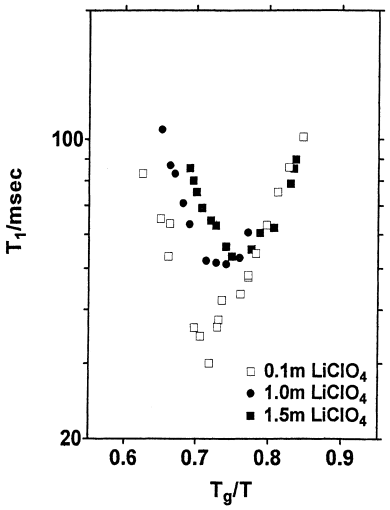

Figure 6 ^{7}Li T_1 relaxation data of *Figure 4a* plotted against reduced temperature, T_g/T. The minimum shifts to lower reduced temperatures as salt concentration is increased, suggesting a progressive decoupling of the ^{7}Li motion from that of the polymer. Error in the points is ± 5%

curves. As previously mentioned, it is not unusual to see asymmetric relaxation curves due to a distribution of correlation times governing the relaxation[41]. In the present data, however, a comparison of low- and high-temperature activation energies in most cases suggests that the relaxation curves are symmetric. The symmetry observed here does not necessarily preclude the existence of a distribution of motional correlation times; however, the curves can be adequately fitted with a single correlation time. The E_a values for ^{7}Li T_1 relaxation in the $LiClO_4$-based SPEs lie in the range 19–27 kJ mol^{-1}, which is consistently higher than in the $LiCF_3SO_3$-based SPEs (16–19 kJ mol^{-1}). This may be a result of stronger ion dissociation (in agreement with the conductivity results) in the former encouraging a greater degree of coordination between the lithium and the polymer host.

The 0.5 m $LiCF_3SO_3$ sample in *Figure 5b* displays a kink in the low-temperature slope of the relaxation curve, occurring at a temperature of approximately $1.2T_g$, at which the E_a changes from 19.7 kJ mol^{-1} to 7.7 kJ mol^{-1}. Similar behaviour has been reported for a $LiCF_3SO_3$/3PEG complex plasticised with dimethyl formamide (DMF)[21]. The reason for this change in slope of the T_1 curve is yet to be ascertained, but a report[42] of ^{23}Na T_1 relaxation of $NaClO_4$/NaI in PEO/polyacrylamide mixtures demonstrated that as conductivity changed from VTF to Arrhenius behaviour, a kink was observed in the T_1 curve at $1.2T_g$. This is significant not least because it connects the observed n.m.r. behaviour with the conductivity behaviour of the samples. The mode coupling theory of transport processes also predicts a change in behaviour of this type near T_g[42].

Figure 5a shows the mobility of the cation decreasing as $LiClO_4$ concentration increases, as indicated by a shift in the position of the minimum to higher temperatures. This behaviour is consistent with the changes in T_g observed in *Figure 2* (inset). To observe the relative mobility of the ^{7}Li nuclei independent of T_g, and hence independent of the mobility of the polymer host, the relaxation times of *Figure 5a* have been replotted in *Figure 6* as a function of T_g/T (a reduced inverse temperature scale). Represented in this way, it can be seen that the lithium cation mobility becomes progressively decoupled from the motion of the polymer complex (as measured by the d.m.t.a. value of T_g) as salt concentration increases. That is, relative to the overall system, the ^{7}Li ions appear to be moving more rapidly at higher salt concentrations. This is consistent with the previously mentioned notion that at these

concentrations, the anion may be functioning as an additional site for cations to hop to and from.

In both cases, as salt is added, the T_1 relaxation process becomes less effective (T_1 at minimum is longer), with the change occurring most dramatically at lower concentrations of salt. This behaviour reflects a modification of the environment of ^{7}Li nuclei. Previous results have indicated that the ^{7}Li T_1 relaxation process in similar polymer hosts most probably involves an interaction of the lithium cation with the ^{1}H on the polymer backbone[15,16,19]. As salt concentration is increased, therefore, it seems that the cation–polymer distance is also increasing—possibly an indication of greater levels of cation–anion interactions and ionic aggregation at higher salt concentrations. However, given the fact that the minima occur at different temperatures, one should take into account that ion aggregation is in fact temperature-dependent, and that the value of T_1 would be expected to change as the minima shift. Other dipolar interactions involving ^{19}F or other ^{7}Li also need to be considered. If they were to dominate the interaction, however, then the larger values of the T_1 minimum at higher salt concentrations would suggest decreasing levels of salt aggregation, contrary to what has been observed elsewhere[20].

^{7}Li T_2 relaxation time measurements. *Figure 7* shows ^{7}Li T_2 relaxation as a function of reciprocal temperature for a 0.5 m $LiCF_3SO_3$ sample. The T_2 results could only be fitted by a double exponential function, which may be interpreted as the presence of at least two sites for the ^{7}Li ion, one with longer T_2 than the other. This is in contrast to the T_1 measurements, which could be modelled adequately by assuming a single relaxation time. The time scale of the T_1 experiment is considerably longer, however, allowing time for physical exchange of the Li^+ ions between sites and thus an averaging of the environment (with the time scale of the physical exchange somewhere in the range of 20–40 ms). Two-component T_2 relaxation is also observed[23] in the systems containing $LiClO_4$, the results indicating that increases in temperature and the addition of the plasticiser tetraglyme both encourage the formation of the short T_2 species. Kim *et al.*[43] have reported a two-component ^{7}Li T_2 in a $LiClO_4$/PEO–polyetherurethane mixture, attributing one component to cations bound into aggregates (less mobile) and the other to more mobile or 'free' ions, with the number of immobile cations increasing as temperature increased. Similar results have been reported by Greenbaum *et al.*[44]. A consistent temperature dependence of 'free' *versus* aggregated ion concentrations has been observed in vibrational spectroscopic investigations on Li^+ and $Na^+(CF_3SO_3)^-$ in low-molecular-weight PEO and PPO[12,20]. Given that the interaction constant C_2/r^6 can be considerably different for the two sites, it is difficult to estimate their relative mobilities from the respective T_2 values. However, the apparently higher activation energies for the short T_2 species may reflect a lower mobility. It should also be mentioned that lower mobility might be expected for lithium cations which are strongly bound to ether oxygens forming O–Li–O ionic crosslinks, although these are likely to decrease in number with increasing temperature.

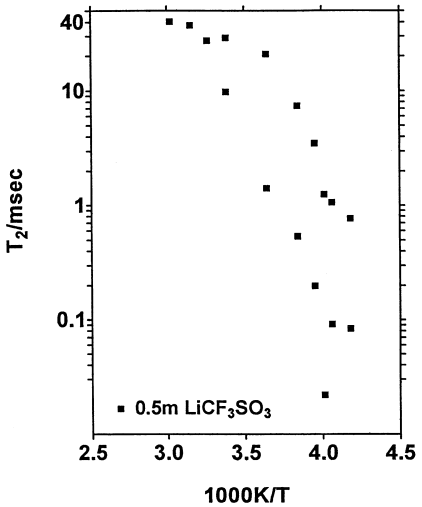

Figure 7 ^{7}Li T_2 relaxation behaviour for a 0.5 m $LiCF_3SO_3$/3PEG sample as a function of temperature, with the presence of two species observed. Error in the points is ± 5%

At higher temperatures the two T_2 components merge, due either to field inhomogeneity or to rapid exchange of the nuclei between spin sites. T_2 approaches the values for T_1 as temperature is increased, suggesting that both T_2 and T_1 relaxation in this sample are modulated by diffusion processes. Below 245 K, T_2 flattens out at a temperature too high ($> T_g$) for the rigid lattice limit, possibly reflecting the slow-down of diffusive motion, with rotation responsible for the fluctuating field causing relaxation. This occurs at the same temperature as the observed kink in the T_1 slope. ^{19}F T_2 results reported previously[21] for the same composition show similar activation energies to the short component of the ^{7}Li T_2 relaxation reported here, again suggesting the presence of an aggregate.

One must also consider, in interpreting the T_1 and T_2 relaxation results discussed above, the possibility that the ^{7}Li nucleus (having a spin number of 3/2) relaxes via interaction with an electric field gradient (quadrupolar relaxation) and the influence this would have on the relaxation phenomenon. So far in this study, no evidence supporting the presence of a strong quadrupolar interaction has been found; however, a combination of isotopic substitution experiments using ^{6}Li salts, multiple field experiments and modelling of the available data will help to discern the extent to which this interaction influences the results presented herein. This will be discussed in greater detail in a forthcoming publication.

CONCLUSIONS

The effect of changing salt concentration and plasticiser addition on the cation environment and mobility in polyether-based polymer electrolytes has been investigated. Both the $LiCF_3SO_3$ and $LiClO_4$ conductivity results exhibited VTF-type temperature dependence, suggesting that charge-carrier diffusion is coupled to free-volume- or configurational-entropy-governed relaxations of the polymer host. The fitting parameter B was unchanged by salt concentration and anion type, reflecting little change in the mechanism of conduction, while the parameter A, related to charge-carrier concentration, increased with increasing salt concentration and was consistently higher in the $LiClO_4$ based system—this latter observation reflecting the stronger dissociation which is also suggested by the ^{7}Li T_1 measurements.

N.m.r. showed that the cationic environment was similar regardless of the nature of the anion, consistent with the invariance in B, although measured activation energies were

lower in the $LiCF_3SO_3$-based SPEs. Furthermore, activation energies determined from conductivity measurements were consistently higher than those obtained from n.m.r. results. This has been observed previously and is likely to be a result of the different time scale of the n.m.r. measurements compared with conductivity measurements. T_1 relaxation measurements provided evidence of ionic aggregation, due either to increasing salt concentration or increasing temperature, or a possible combination of both factors. This aggregation seemed to be more pronounced with changes occurring at lower salt concentrations (< 1.0 M): an observation consistent with molar conductivity behaviour as a function of salt concentration[20].

The correlation between the structural glass transition temperature, as measured by d.m.t.a., and the mobility of individual ionic species is critical when interpreting conductivity and n.m.r. behaviour. Increasing salt concentration reduces the T_g of the polymer/salt complex and this change in mobility is a primary factor influencing the conductivity as the salt concentration increases. Interestingly, although ^{7}Li n.m.r. relaxation times in general reflected these changes in T_g by a shift in position of the T_1 minimum, the mobility of the Li cation is seen to be progressively decoupled from the mobility of the salt/polymer complex. This suggests a shift to a mechanism which may involve lithium ions transitting between aggregates; the mobility of such lithium ions is therefore less influenced by large-scale polymer-chain motions. D.m.t.a. also indicated a changing heterogeneity of the system as both salt and tetraglyme were added; tetraglyme in particular broadened the distribution of relaxation times, possibly due to the formation of microdomains.

ACKNOWLEDGEMENTS

This work has been made possible by an Australian Postgraduate Award, and assistance from an Australian Research Council grant, a British Council Bursary and the Basque Government.

REFERENCES

1. Fenton, D. E., Parker, J. M. and Wright, P. V., *Polymer*, 1973, **14**, 589.
2. Armand, M. B., Chabagno, J. M. and Duclot, M., in *Fast Ion Transport in Solids*, eds Vashishta, Mundy and Sheroy, Elsevier, North Holland, 1979.
3. Armand, M. B., *Annu. Rev. Mater. Sci.*, 1986, **4**, 245.
4. Gray, F. M., *Solid Polymer Electrolytes: Fundamentals and Technological Applications*. VCH Publishers, New York, 1991.
5. Bruce, P. G. and Vincent, C. A., *J. Chem. Soc. Faraday Trans.*, 1993, **89**, 3187.
6. MacCallum, J. R. and Vincent, C. A. (Eds.), *Polymer Electrolytes Reviews I*. Elsevier, London, 1987.
7. MacFarlane, D. R., Sun, J., Forsyth, M., Bell, J. M., Evans, L. A. and Skyrabin, I. L., *Solid State Ionics*, 1996, **86-88**, 959.
8. Berthier, C., Gorecki, W., Minier, M., Armand, M. B., Chabagno, J. M. and Rigaud, P., *Solid State Ionics*, 1983, **11**, 91.
9. Minier, M., Berthier, C. and Gorecki, W., *J. Phys.*, 1984, **45**, 939.
10. Ratner, M. A., in *Polymer Electrolyte Reviews I*, eds J. R. MacCallum and C. A. Vincent. Elsevier, London, 1987, Ch. 7.
11. Souquet, J. L., Duclot, M. and Levy, M., *Solid State Ionics*, 1996, **85**, 149.
12. Torell, L. M., Jacobsson, P. and Petersen, G., *Polym. Adv. Tech.*, 1993, **4**, 152.
13. Schantz, S., Torell, L. M. and Stevens, J. R., *J. Chem. Phys.*, 1991, **94**, 6862.
14. Forsyth, M., Meakin, P. and MacFarlane, D. R., *Electrochim. Acta*, 1995, **40**, 2339.
15. Forsyth, M., MacFarlane, D. R., Meakin, P., Smith, M. E. and Bastow, T. J., *Electrochim. Acta*, 1995, **40**, 2343.
16. Ali, F., Forsyth, M., Garcia, M., Smith, M. E. and Strange, J. H., *J. Solid State NMR*, 1995, **5**, 217.
17. Forsyth, M., Smith, M. E., Meakin, P. and MacFarlane, D. R., *J. Polym. Sci., Part B*, 1994, **32**, 2077.
18. MacFarlane, D. R., Sun, J., Meakin, P., Fasoulopoulos, P. and Hey, J., *Electrochim. Acta*, 1995, **40**, 2131.
19. Forsyth, M., Meakin, P., MacFarlane, D. R., Bulmer, G. and Reid, M., *J. Mater. Chem.*, 1994, **4**, 1149.
20. Bishop, A. G., MacFarlane, D. R., McNaughton, D. and Forsyth, M., *J. Phys. Chem.*, 1996, **100**, 2237.
21. Forsyth, M., Garcia, M., MacFarlane, D. R., Ng, S., Smith, M. E. and Strange, J., *Solid State Ionics*, 1996, **86-88**, 1365.
22. Forsyth, M., Garcia, M., MacFarlane, D. R., Meakin, P., Ng, S. and Smith, M. E., *Solid State Ionics*, 1996, **85**, 209.
23. Ng, S. T. C., Forsyth, M., MacFarlane, D. R., Garcia, M., Smith, M. E. and Strange, J., *Electrochim. Acta*, in press.
24. Jolliffe, C., personal communication (see also Honours Thesis, Monash University, 1996).
25. Ng, S. T. C., Jolliffe, C., Goodwin, A. and Forsyth, M., *Electrochim. Acta*, in press.
26. McCrum, N. G., Buckley, C. P. and Bucknall, C. B., *Principles of Polymer Engineering*. Oxford Science Publications, Oxford, 1991.
27. Le Nest, J. F., Gandini, A. and Cheradame, H., *Br. Polym. J.*, 1988, **20**, 253.
28. Utracki, L. A., in *Polymer Alloys and Blends: Thermodynamics and Rheology*. Oxford Science Publications, Oxford, 1988.
29. Sukeshini, A. M., Nishimoto, A. and Watanabe, M., *Solid State Ionics*, 1996, **86-88**, 385.
30. Watanabe, M., Oohashi, S., Sanui, K., Ogata, N., Kobayashi, T. and Ohtaki, Z., *Macromolecules*, 1985, **18**, 1945.
31. Killis, A., Le Nest, J. F., Gandini, A. and Cheradame, H., *Macromolecules*, 1984, **17**, 63.
32. Watanabe, M., Sanui, K., Ogata, N., Kobayashi, T. and Ohtaki, Z., *J. Appl. Phys.*, 1985, **57**, 123.
33. Le Nest, J. F., Gandini, A. and Cheradame, H., *Br. Polym. J.*, 1988, **20**, 253.
34. Boden, N., Leng, S. A. and Ward, I. M., *Solid State Ionics*, 1991, **45**, 261.
35. Arumugam, S., Shi, J., Tunstall, D. P. and Vincent, C. A., *J. Phys.: Condens. Matter*, 1993, **5**, 153.
36. Ferry, A., Jacobson, P. and Torell, L. M., *Electrochim. Acta*, 1995, **40**, 2369.
37. Forsyth, M., Payne, V. A., Ratner, M. A., de Leeuw, S. W. and Shriver, D. F., *Solid State Ionics*, 1992, **53-56**, 1011.
38. Wetton, R. E., in *Developments in Polymer Characterisation—5*, ed. J. V. Dawkins. Elsevier Applied Science, London, 1986.
39. Bloembergen, N., Purcell, E. M. and Pound, R. V., *Phys. Rev.*, 1948, **73**(7), 679.
40. Chung, S. H., Jeffrey, K. R. and Stevens, J. R., *J. Chem. Phys.*, 1991, **94**(3), 1803.
41. Connor, T. M., *Trans. Faraday Soc.*, 1963, **60**, 1574.
42. Wieczorek, W., Such, K., Chung, H. and Stevens, J. R., *J. Phys. Chem.*, 1994, **98**, 9047.
43. Kim, D. W., Park, T. K., Rhee, H. W. and Kim, H. D., *Polym. J.*, 1994, **26**, 493.
44. Greenbaum, S. G., Pat, Y. S., Wintersgill, M. C. and Fontanella, J. J., *Solid State Ionics*, 1988, **31**, 242.